JCB

Riedel et al., https://doi.org/10.1083/jcb.201705068



A

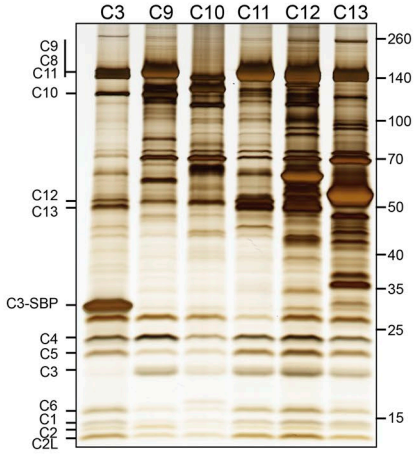


B

| Protein | Complex | C3 | C10 | C3 | C9 | C11 | C13 |
|---|---|---|---|---|---|---|---|
| C11 | • | 95 | | 287 | | 1330 | 240 |
| C9 | • | 143 | 157 | 310 | 1040 | | |
| C8 | • | 70 | | 256 | | 813 | 222 |
| C10 | • | 58 | 415 | 195 | 288 | | |
| C12 | • | 46 | | 230 | 15 | 581 | 154 |
| C13 | • | 21 | | 131 | | 362 | 829 |
| C4 | • | 32 | 12 | 149 | 48 | 168 | 121 |
| C5 | • | 22 | 13 | 196 | 119 | 161 | 96 |
| C3 | • | 124 | 14 | 778 | 123 | 118 | 159 |
| C6 | • | 3 | | 133 | 7 | 28 | 43 |
| C2 | • | 2 | 3 | 126 | 58 | 19 | 35 |
| C1 | • | 25 | 8 | 97 | 39 | 47 | 43 |
| C2L | • | 2 | | 17 | 4 | 6 | 3 |
| Sec31 | | | | 5 | | | |
| Sec13 | | | | 4 | | | |

C

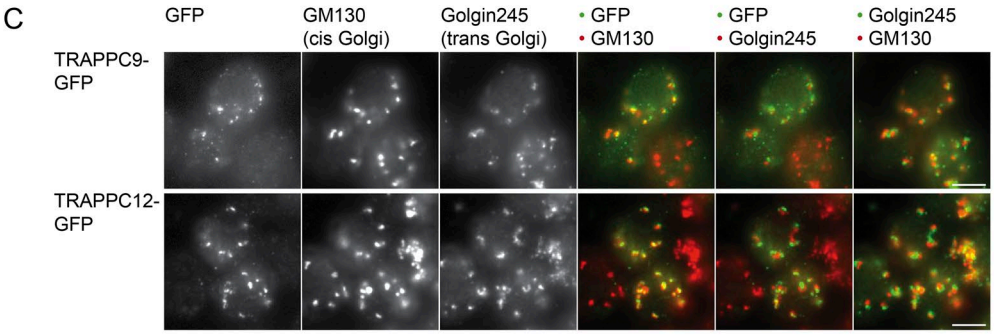


D

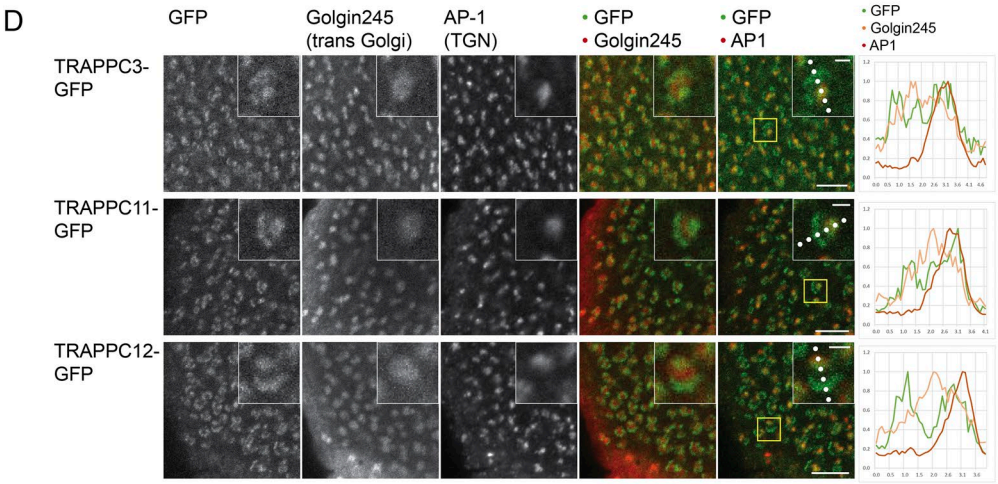


Figure S1. **SBP-GFP–tagged TRAPP complex subunits in *Drosophila* S2 cells. (A)** Silver-stained protein gel of TRAPPC3, TRAPPC9, TRAPPC10, TRAPPC11, TRAPPC12, and TRAPPC13 tandem affinity–purified from stably transfected cell lines. Molecular masses are given in kilodaltons. **(B)** Mass spectrometry analysis of proteins associated with TRAPPC3, TRAPPC9, TRAPPC10, TRAPPC11, and TRAPPC13 after TAP from stably transfected S2 cells. Total spectral counts for each protein are shown, with these experiments being independent biological replicates of those in Fig. 2 A. **(C)** Widefield micrographs of SBP-GFP–tagged TRAPPC12 and TRAPPC9 transiently expressed in S2 cells that were then stained for GFP and the Golgi markers Golgin245 and GM130. **(D)** Confocal micrographs of SBP-GFP–tagged TRAPPC3, TRAPPC11, and TRAPPC12 in salivary glands from wandering third instar larvae and stained for GFP, Golgin245, and the γ subunit of the AP-1 clathrin adapter. Line scans are from representative Golgi stacks (dotted lines on GFP/AP-1 panels). The trans peak in the TRAPP bimodal distribution closely overlaps the TGN marker. Bars: (main images) 5 µm; (insets) 1 µm. Images in C and D are representative of at least two independent experiments, with at least three micrographs obtained from each.

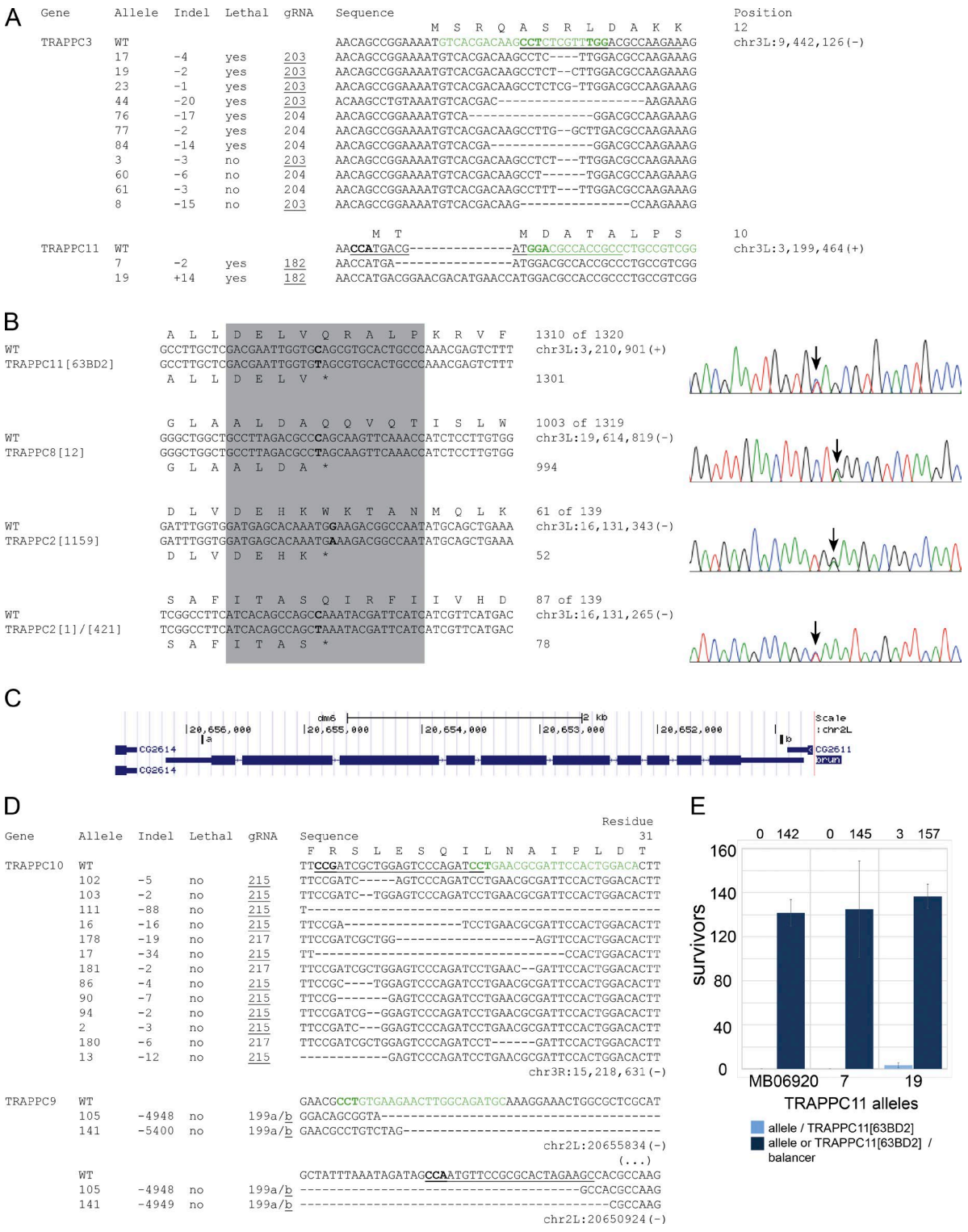


Figure S2. **Sequence details of EMS alleles in various TRAPP complex subunits. (A)** Sequence details of alleles carrying indels in either TRAPPC3 and TRAPPC11. Sequences corresponding with the two guide RNAs used for each gene are indicated in the WT sequence (green and underlining, respectively). **(B)** Sequence analysis to reveal the genetic lesion in previously reported EMS alleles of TRAPP subunit genes (Fig. 4 A). The sequencing traces for the area in gray are to the right of each sequence. Arrows show residues that were altered in the mutant allele. Note that for TRAPPC8, the trace is for the complementary strand. Black, G; blue, C; green, A; red, T. **(C)** Graphical representation of the gene model of TRAPPC9 (*brunelleschi*). The positions of the guide RNAs 199a and 199b used to generate the deletion alleles TRAPPC9[105] and TRAPPC9[141] are indicated above the gene model. The image was generated with the UCSC genome browser. **(D)** Sequence details of alleles carrying indels in TRAPPC10 (top) or alleles carrying a deletion of the whole coding sequence in TRAPPC9 (bottom). Sequences corresponding with the two guide RNAs used for each gene are indicated in the WT sequence (green and underlining, respectively). Only the genomic region of TRAPPC9 to which the guide RNAs bind is shown. **(E)** TRAPPC11[63BD2]/TRAPPC11[19] heterozygotes in rare cases develop into adulthood, and TRAPPC11[63BD2]/TRAPPC11[MB06920] and TRAPPC11[63BD2]/TRAPPC11[7] heterozygotes do not. The bars show the mean number of adult progeny obtained from two parallel crosses. The mean value is shown above each bar. Error bars show SD.

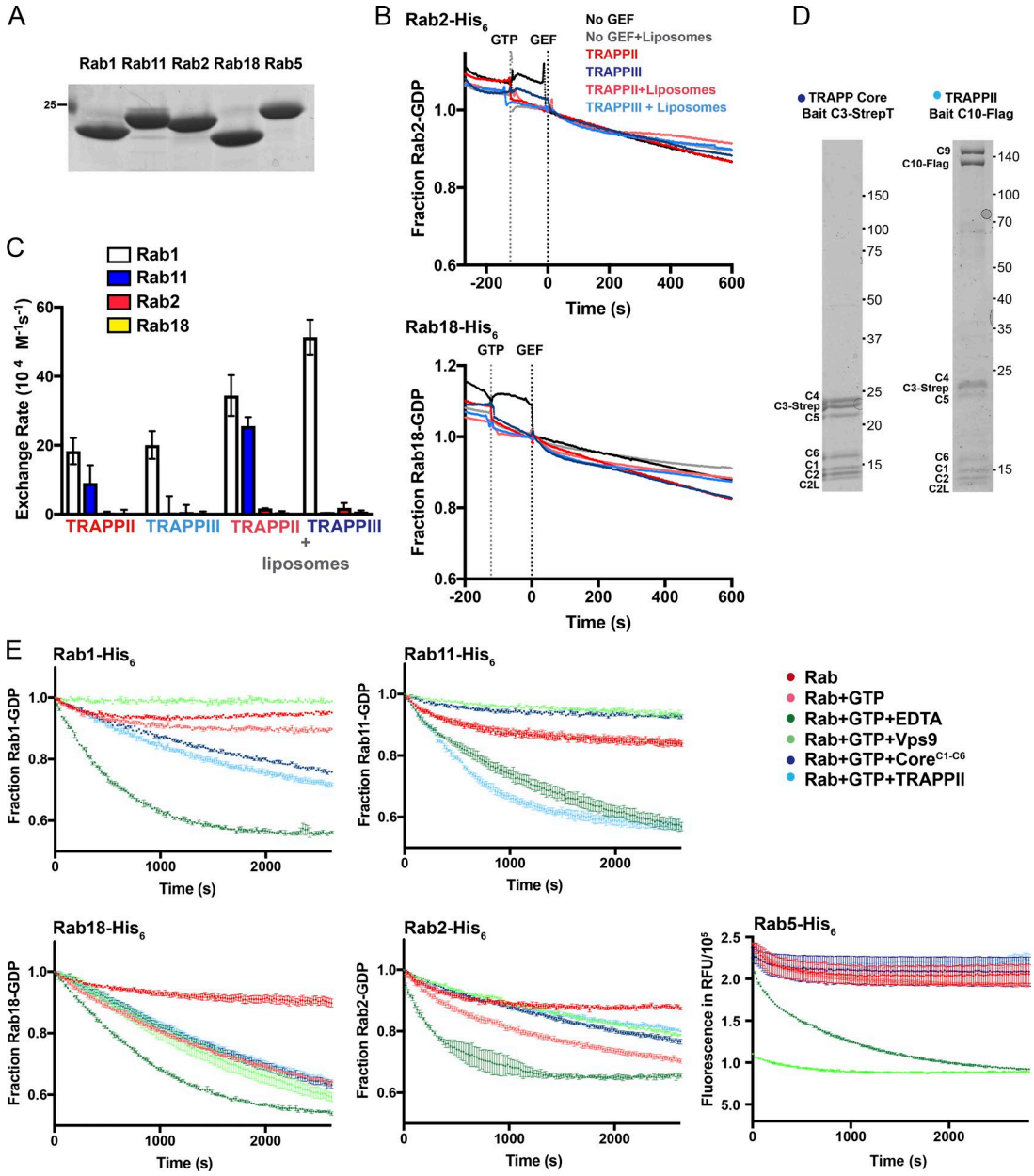


Figure S3. **Rab GEF assays with recombinant TRAPP complexes. (A)** 1 µg of $His_6$-tagged Rab substrates used in the GEF assays assessed by SDS-PAGE and Coomassie staining. **(B)** GEF assays of the two Golgi-associated Rabs, Rab2 and Rab18. Traces show means of three experiments. Both Rabs have high intrinsic exchange rates that did not change when either TRAPPII or TRAPPIII were present in the reaction. **(C)** Comparison of the TRAPP complexes effect on mant-GDP release from Rab1, Rab11, Rab2, and Rab18. Shown is the mean exchange rate from three experiments for each substrate with either TRAPPII or TRAPPIII alone or in the presence of synthetic Golgi liposomes. **(D)** Purified TRAPP complexes used for GEF assays. The purified material was run in SDS-PAGE gel. Molecular masses are given in kilodaltons. **(E)** GEF assays performed in triplicate in 96-well plate format. Rabs were loaded with mant-GDP, and change in fluorescence was measured over time after addition of a GEF or EDTA. Rabs showed a slow nucleotide release exchange in the absence of GTP. In the presence of GTP, Rab1 and Rab11 showed a slow exchange similar to the one in the absence of GTP, whereas the exchange rate on Rab2 and Rab18 was more rapid, indicating a higher intrinsic rate of nucleotide loss. All Rabs showed a pronounced mant-GDP release when 10 mM EDTA was added to the reaction. The VPS9 domain of Rabex5, which works as a strong activator of Rab5, did not have activity on the other Rabs. Error bars show SEM.

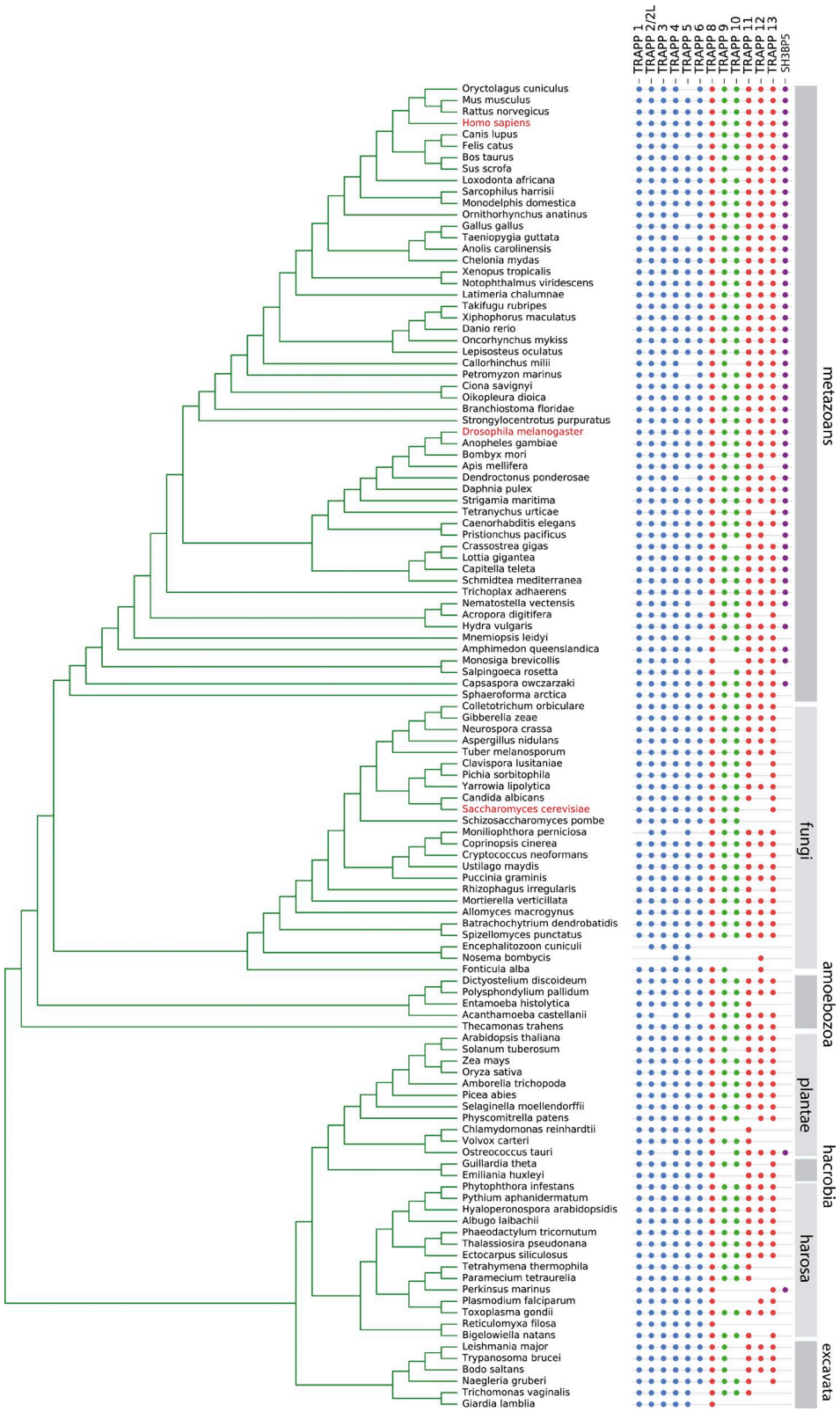


Figure S4. **Evolutionary conservation of TRAPP complex subunits and Parcas/SH3BP5.** Colored circles indicate the presence of a predicted orthologue in each species. Orthologues were identified using HMM profile searches based on a profile constructed using phmmr reciprocal best hits (Eddy, 2011) and then expanded in stages as further proteins were detected using hmmsearch, accepting sequences that reciprocally found the query or a close paralog (>97% identity) until no further sequences were detected. Searches were started using TRAPP subunits from human, *Drosophila*, *Arabidopsis thaliana*, and *Yarrowia lipolytica* as well as the hits combined. The dendrogram of species showed consensus phylogenetic relationships, but the length of the branches did not carry meaning. Parcas/SH3BP5 orthologues were found in only two of the nonmetazoan species, but these hits appeared correct as they could be confirmed using Pfam and *jackhmmer* (Finn et al., 2015). It is possible that these arose from horizontal gene transfer.

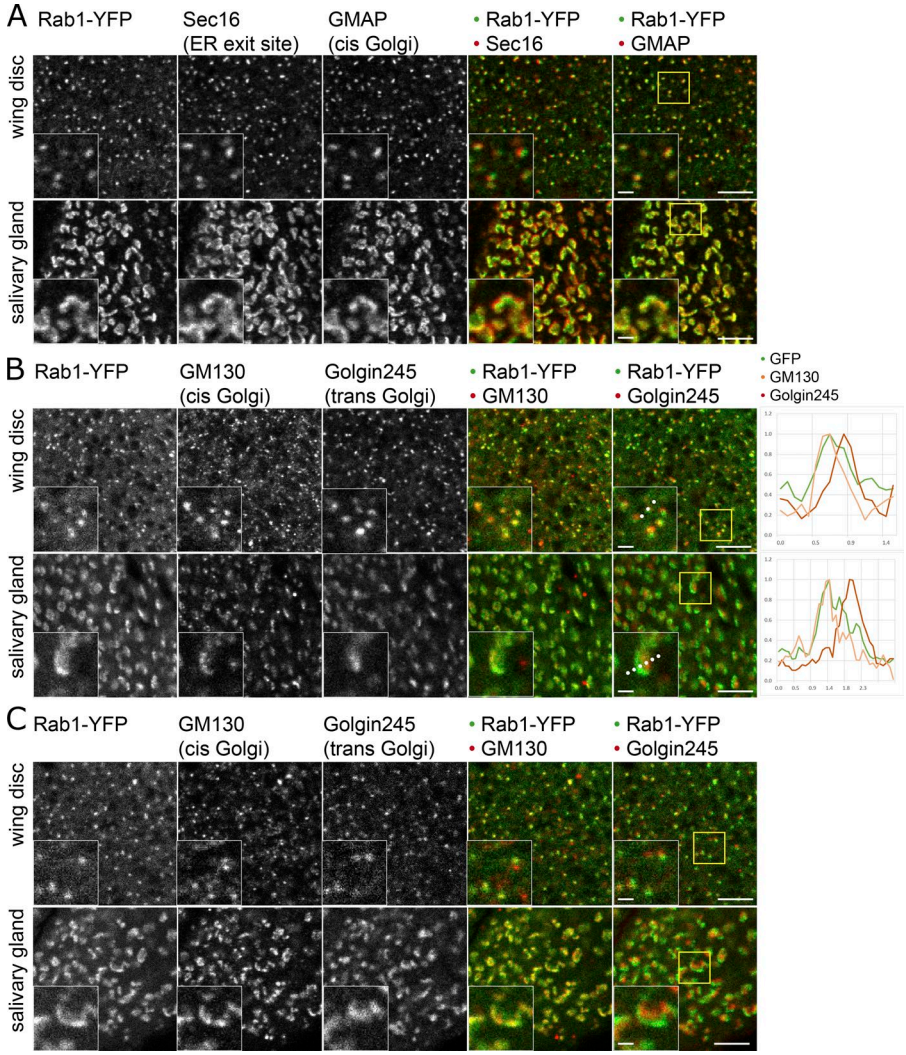


Figure S5. **Localization of Rab1 in WT and TRAPPC9 mutant larval tissues. (A and B)** Confocal micrographs of YFP-tagged Rab1 in wing imaginal discs and salivary glands dissected from wandering third instar larvae and stained for GFP and the indicated Golgi or ER exit site markers. Line scans are from representative Golgi stacks (dotted lines in Rab1-YFP/Golgin245 panels). Rab1-YFP was found at the cis side of the Golgi. **(C)** Confocal micrographs of YFP-tagged Rab1 in wing imaginal discs and salivary glands dissected from third instar TRAPPC9[105] homozygous mutant larvae and stained for GFP, GM130, and Golgin245. Bars: (main images) 5 µm; (insets) 1 µm. Images are representative of at least two independent experiments, with at least three micrographs obtained from each.

## References

Eddy, S.R. 2011. Accelerated profile HMM searches. *PLOS Comput. Biol.* 7:e1002195. https://doi.org/10.1371/journal.pcbi.1002195

Finn, R.D., J. Clements, W. Arndt, B.L. Miller, T.J. Wheeler, F. Schreiber, A. Bateman, and S.R. Eddy. 2015. HMMER web server: 2015 update. *Nucleic Acids Res.* 43(W1):W30–W38. https://doi.org/10.1093/nar/gkv397